LateralPaD: A Surface-Haptic Device That Produces Lateral Forces on A Bare Finger

Xiaowei Dai[‡]*, J. Edward Colgate*, Michael A. Peshkin*

[‡]State Key Lab of Virtual Reality Technology and Systems, Beihang University,
37 Xueyuan Rd, Haidian District
Beijing, 100191, China

*Northwestern University
2145 Sheridan Rd
Evanston, IL, 60208, USA

Abstract

The LateralPaD is a surface haptic device that generates lateral (shear) force on a bare finger, by vibrating the touch surface simultaneously in both out-of-plane (normal) and in-plane (lateral) directions. A prototype LateralPaD has been developed in which the touch surface is glass, and piezoelectric actuators drive normal and lateral resonances at the same ultrasonic frequency (~22.3 KHz). The force that develops on the finger can be controlled by modulating the relative phase of the two resonances. A 2DOF load cell setup is used to characterize the dependence of induced lateral force on vibration amplitude, relative phase, and applied normal force. A Laser Doppler Vibrometer (LDV) is used to measure the motion of glass surface as well as of the fingertip. Together, these measurements yield insight into the mechanism of lateral force generation. We show evidence for a mechanism dependent on tilted impacts between the LateralPaD and fingertip.

Keywords: Surface haptic, lateral force

Index Terms: H.5.2 [Information Systems]: User Interfaces-Haptic I/O

1 Introduction

Lateral forces can be used to create the illusion of texture and surface features [1-2]. Several surface haptic devices have been developed to take advantage of this illusion. Takasaki et al. [3] used surface acoustic waves (SAW) to reduce the effective friction on a slider. A disadvantage of a slider-based device is that it does not operate on a bare finger. Watanabe and Fukui [4] developed the first ultrasonic vibrating plate capable of controlling the surface roughness displayed to a bare finger. The ultrasonic vibrating frequency was 75.6 KHz and the normal vibration amplitude was about 2 microns. Subjects reported a "smoother" feeling. Biet et al. [5] used an array of piezoelectric actuators glued to the underside of a metallic sheet to generate out-of-plane vibrations with 1 micron amplitude and found that frictional forces could be modulated continuously by adjusting the amplitude of the vibration. Winfield et al. [6] developed the Tactile Pattern Display (TPaD) capable of varying the surface friction between the finger and a glass plate vibrating at approximately 30 KHz with an amplitude of 4 microns.

While these devices reduced friction, others have used electrostatic force to increase friction. Yamamoto et al. [7] designed an electrostatic tactile display consisting of a thin conductive film slider with stator electrodes that excite electrostatic attraction forces between the slider and the stator. Bau et al. [8] developed tactile feedback by modulating the electrostatic force between finger and touchpad surface, and a number of other similar devices have also been reported.

In an effort to produce active forces on the fingertip, Biet et al. [9] developed a Travelling Lamb Wave tactile display using the stator of a Travelling Wave Ultrasonic Motor that operated at a resonant frequency of around 40 KHz. The authors modeled the lateral stretching force as proportional to the relative velocity between finger and the surface but stopped short of demonstrating active forcing.

Chubb et al. [10] introduced the ShiverPaD, which took advantage of out-of-plane and in-plane motion of a touched surface to generate shear force on a bare finger. ShiverPaD used 39 KHz out-of-plane vibrations to modulate the friction coefficient between finger and glass surface. The glass surface was also oscillated laterally at a much lower frequency, 854 Hz. By modulating friction (via the 39 KHz) within each 1/854 sec cycle of lateral vibration, a net lateral force was produced. Shear forces in excess of 80mN were reported. The 854 Hz in-plane oscillation, however, led to audible noise.

In this paper, the LateralPaD is introduced. The LateralPaD can generate active lateral forces on a bare finger contacting a glass surface. Out-of-plane and in-plane vibrations are arranged to have coinciding resonant frequencies of 22.3 KHz, supporting a tilted straight-line motion of the glass surface or elliptical motions. Tilted straight-line motions interact with the fingertip to produce lateral force. The next section describes the construction of the LateralPaD prototype. Section 3 presents four experiments that characterize the performance of the LateralPaD as a function of several key parameters. Section 4 presents two more experiments that aim to elucidate the mechanism by which force is generated. Force production is discussed in Section 5, and Section 6 presents a simple application, a virtual environment in which lateral force is a function of fingertip position. Section 7 presents conclusions and some considerations for future work.

2 Prototype Design

Our LateralPaD prototype is a 22 mm x 76 mm x 2.3 mm glass plate driven by two sets of piezoelectric actuators (henceforth, "piezos"). Two piezo disks glued to the top surface of the glass excite a bending resonance for out-of-plane motion (Figure 3a),

daixw@northwestern.edu
colgate@northwestern.edu
peshkin@northwestern.edu

IEEE Haptics Symposium 2012
4-7 March, Vancouver, BC, Canada
978-1-4673-0809-0/12/$31.00 ©2012 IEEE

and piezo stacks at either end excite an in-plane resonance (Figure 3b). Out-of-plane motion will be referred to as "**normal vibration**" and in-plane motion will be referred to as "**lateral vibration**." Figure 1 shows the LateralPaD on a 2DOF load cell setup. The whole structure is shown in Figure 2. In this figure, the light yellow rectangular region is the useful workspace where significant shear force can be developed. Finger position is measured with a projected capacitance sensor, visible as the green circuit board underneath the glass touch surface in Figure 1. (This sensor is not integrated to the glass, and is not transparent.)

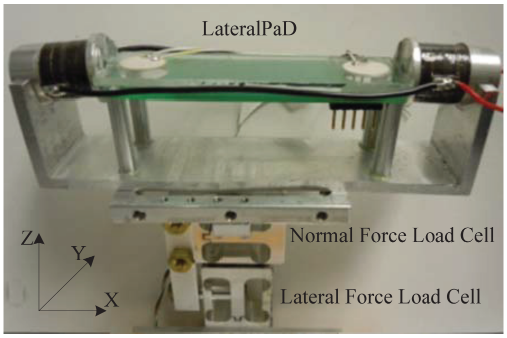

Figure 1. LateralPaD and 2DOF load cell setup

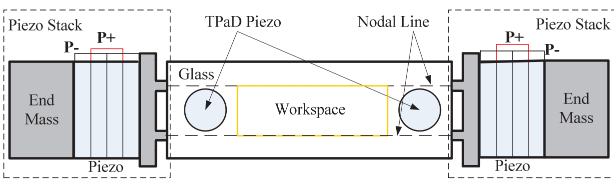

Figure 2. Top view of the LateralPaD structure

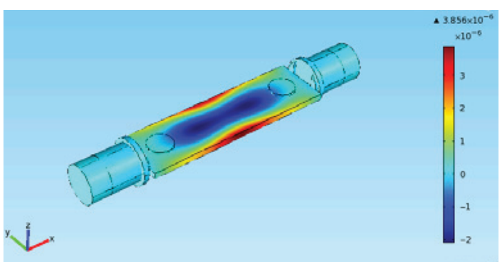

(a) Displacement of normal vibration in the Z axis

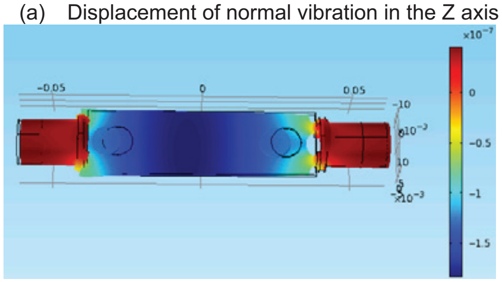

(b) Displacement of lateral vibration in the X axis

Figure 3. Normal and lateral vibration simulation of the LateralPaD

Figure 3a illustrates the bending mode as predicted by a finite element package (COMSOL). There are two nodal lines where the displacement is almost zero. These nodal lines run roughly parallel to the long edges of the glass, and together with the piezo disks, form the boundaries of the useful workspace. Figure 3b illustrates a longitudinal resonance, driven by the two piezo stacks, which is used to generate lateral vibratory motion. In this case, nodal lines occur roughly at the ends of the glass plate. To minimize interaction between the lateral and normal dynamics, the piezo stacks are glued to the glass plate at the ends of the bending mode nodal lines. These locations are also used for mounting. The frequency of the lateral resonance is very sensitive to the length of the glass and the piezo stack. We adjusted the end-masses to arrange that the resonant frequency for lateral vibration matched the resonant frequency for normal vibration. Drive signals for the two sets of piezos originated from the same signal source (Analog Devices AD9959) and are therefore at the same frequency. We could vary the amplitude of each signal, and the phase difference between them.

3 LATERAL FORCE MEASUREMENT

When a bare finger was placed in contact with the LateralPad, a lateral force was developed. We measured its dependence on vibration amplitude in the normal direction, vibration amplitude in the lateral direction, and relative phase between these two vibrations. We also measured its dependence on the normal force applied by the user's finger. To make these measurements, the LateralPaD was mounted on a 2DOF force measurement rig composed of two load cells stacked together, one aligned for normal force and the other for lateral force (Figure 1). In the following figures, black curves are the average, and error bars denote standard deviation, over multiple trials. Wherever motion amplitudes are reported, they were obtained with a Polytec PSV-400 scanning Laser Doppler Vibrometer (LDV).

A number of the experimental results are reported in terms of a "lateral force coefficient" defined as:

$$\mu_L = \frac{f_{Lateral}}{f_{Normal}} \tag{1}$$

The lateral force coefficient affords comparison with the friction coefficient. Notably $f_{Lateral}$ is an active force that can push a non-moving fingertip, or even push a fingertip in the direction that it is already moving. Friction modulation devices can only produce force that opposes motion of the fingertip.

<u>Experiment 1 – Friction Reduction</u>

To provide a baseline of comparison, an initial experiment was performed in which only the "normal vibration" piezos were activated. Acting here as a TPaD [5], the device is capable of reducing friction, but not of generating active forces. One of us (XD) dragged his index finger across the glass surface with almost constant normal force and velocity while recording normal and lateral forces at 100 Hz. Thirty rightward swipes and thirty leftward swipes were averaged to compute each data point. Data points for which normal force was less than 0.1 N was excluded, as were also the first 10 and last 10 samples of each swipe. With practice the normal force could be held steady at approximately 0.27 N (standard deviation of 0.04 N.) Figure 4 shows that the friction coefficient drops from 0.48 to about 0.06, with increasing normal motion amplitude.

While previous publications (including ours) have explained this friction reduction in terms of a squeeze film of air, we will show later in this paper that periodic contact is also implicated. The existence of periodic contact is important for explaining the operation of the LateralPaD.

<u>Experiment 2 – Dependence on Phase</u>

A second experiment examined the range of lateral force coefficients that could be produced. Peak-to-peak voltages across the piezo disks (normal vibration) and piezo stack (lateral vibration) were set to 98 V and 192 V respectively, and forces were measured as a function of relative phase. During the measurement, the finger was maintained in static contact with the glass surface and an effort was made to maintain the normal force steady and keep the normal force at the same level as that in experiment 1. In this experiment, the average normal force was about 0.26 N and standard deviation was about 0.03 N. At each value of relative phase, 900 points were collected at 100 Hz and an average and standard deviation were computed.

Figure 5 shows the results: the relative phase modulates both the magnitude and direction of the lateral force. Maximum lateral force coefficient is obtained at a phase of about 200° for positive force and 20° for negative force. The peak lateral force coefficient is about 0.13, considerably less than the maximum friction coefficient (0.48).

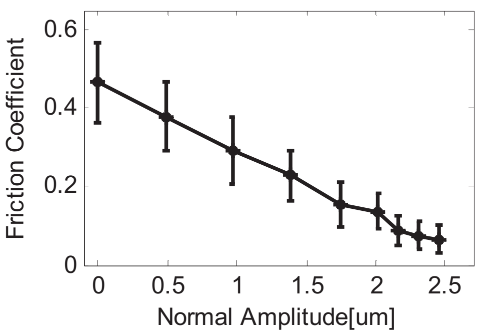

Figure 4. Friction coefficient between finger and glass surface when only the bending mode is activated

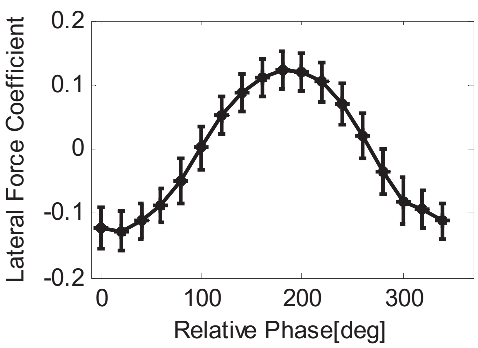

Figure 5. Lateral force coefficient versus relative phase

Experiment 3 – Dependence on Vibration Amplitude

In this experiment, the dependence of the lateral force coefficient on normal vibration amplitude and lateral motion amplitude was explored. The finger was held in static contact with the glass surface and the normal force was held steady at about 0.31 N (standard deviation of 0.04 N). The relative phase of the two driving voltages was set to 20°. At each drive voltage, 900 points were collected and an average and standard deviation were computed. Figure 6 shows the results for a set of trials in which the voltage across the piezo stack (lateral vibration) was set to 192V peak-to-peak, and the voltage across the piezo disks was varied from 0 to 98V peak-to-peak. In each case, the normal vibration amplitude was measured with the LDV. Over the range tested, the lateral force coefficient grows with normal vibration amplitude at a greater than linear rate.

Figure 7 shows the results for a set of trials in which the piezo disk voltage (normal vibration) was set to 98 V peak-to-peak and the piezo stack voltage was varied from 0 to 192 V peak-to-peak. It is difficult to measure lateral vibration amplitude (see Experiment 6), so data are simply reported as a function of voltage. This plot shows that lateral force coefficient grows with lateral excitation, but less than linearly. A direct measure of lateral vibration amplitude would be needed, however, to draw further conclusions.

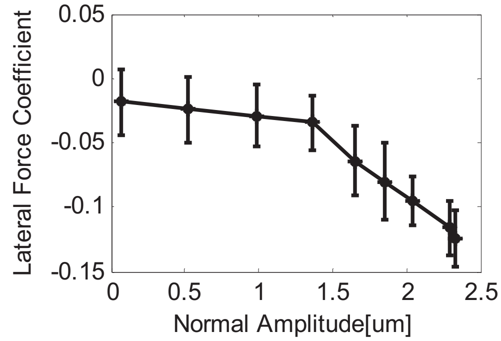

Figure 6. Lateral force coefficient versus normal vibration amplitude

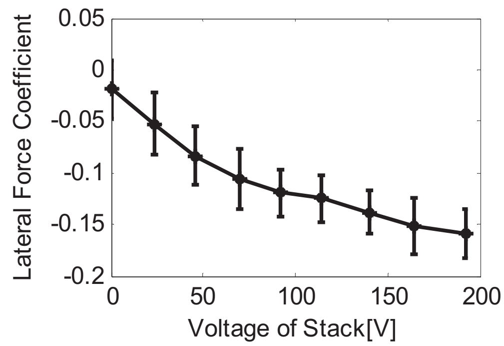

Figure 7. Lateral force coefficient versus piezo stack voltage

Experiment 4 – Dependence on Normal Force

Here the experimenter varied the normal force of his index finger on the glass plate. The finger was held in static contact with the glass surface, the piezo voltages were set to 98 V (normal vibration) and 192 V (lateral vibration) peak-to-peak, and the relative phase was set to 20°. Figure 8a shows that the lateral force increased with normal force, but not quite linearly. As a consequence, the lateral force coefficient decreases with increasing normal force (Figure 8b). We do not think the variation is due to a decrease of normal vibration amplitude with normal force, because LDV data shows that normal forces less than 1 N have almost no effect on normal vibration amplitude.

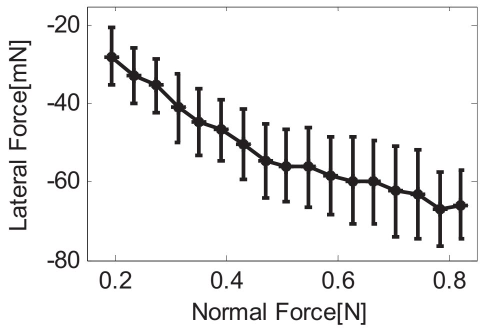

(a) Lateral force versus normal force

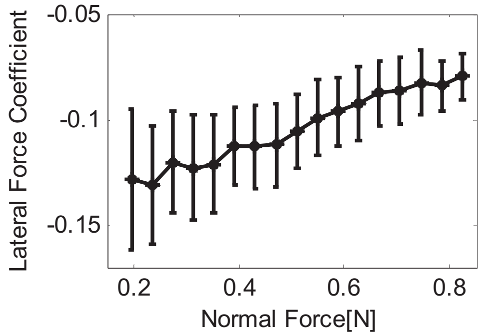

(b) Lateral force coefficient versus normal force

Figure 8. Lateral force and lateral force coefficient versus normal force

4 MECHANISM OF FORCE GENERATION

The above force experiments characterize the performance of the LateralPaD, illustrate how the relative phase and amplitude of normal and lateral vibration modulate the lateral force coefficient, and show how normal force affects the lateral force, but they do not illuminate the *mechanism* of force generation. We had originally believed that the combination of normal and lateral vibration would cause an elliptical surface motion which would repeatedly drag across the skin of the fingertip, producing a lateral force. This mechanism, however, would not seem to predict the observed increase of lateral force coefficient with normal vibration amplitude (Figure 6). The lateral force due to dragging should depend on the average normal force during contact. We would expect this to depend on the normal force applied by the finger and not on the normal vibration amplitude, although it is possible that suction occurring during finger-surface separation would cause amplitude dependence. To gain additional insight, motion measurements were made with the LDV. Experiment 5 focused on measuring fingertip interaction with the TPaD and LateralPaD, and Experiment 6 focused on measuring both the normal and lateral components of LateralPaD surface vibration.

<u>Experiment 5 – Motion of Finger vs. Surface – Normal Direction</u>

In this experiment, velocity of both the fingertip and the glass surface were measured, in the normal direction only. While the LDV can be used to make displacement measurements, it is difficult to remove low frequency noise such as building vibrations and unsteady hands. Instead, velocity measurements were integrated over short time periods to estimate displacement. For the data reported here, the sampling frequency was 1.024 MHz.

We aimed the LDV's laser downward toward the top surface of the LateralPaD (Figure 9). To measure surface motion, a small section of the lower surface of the glass was painted with a silver marker. To measure skin motion, the fingertip was also painted with a silver marker and placed, facing upward, on the lower surface of the glass. The LateralPaD was mounted on the force sensing setup described earlier. Representative velocity data are the black plots in Figure 10. The blue plots are position estimates obtained by integrating the velocity data. Because the fingertip and surface motions were not measured simultaneously, the voltage excitation signal for the piezo disks was also recorded as a reference signal, and then in post-processing used to align the fingertip and surface motions with respect to excitation phase. It became apparent that there were, in every case, times during which the finger and glass velocities closely tracked one another. This is shown in Figure 10a (dashed ellipse). Because this period is preceded by a period in which the velocity of the fingertip drops quite precipitously as if a collision had occurred, we assume that these are instances of contact, or at least very close to contact. This information was used to align the displacement plots vertically (integration of velocity cannot establish the offset in displacement.)

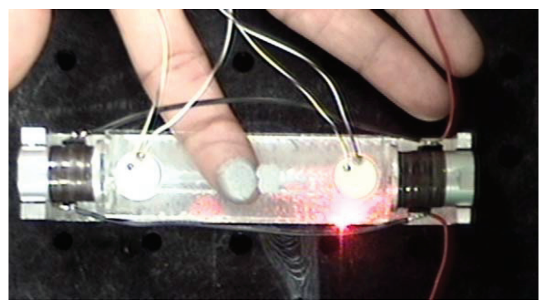

Figure 9. Apparatus for measuring glass and fingertip motion

Figure 10 shows the results at two different normal vibration amplitudes, both with an average normal force of about 0.5N. These are interesting data in part because they contradict a long-held assumption (ours as well as others') that friction reduction occurs because the fingertip “floats” on a squeeze film of air [3, 6, 11]. In every case, collision appears to occur. This does not mean that no squeeze film exists, only that the finger does not entirely float on a squeeze film. Indeed, Figure 10c provides strong evidence that a squeeze film does exist: in every second cycle, the finger reverses direction in the absence of a collision. Thus, one reasonable explanation for friction reduction is that, as the normal vibration amplitude increases, the finger is increasingly supported by a squeeze film and decreasingly supported by contact. This hypothesis will be explored further in future work. For now we note only a confusing disparity: one would presume that when a finger is supported more by a squeeze film and less by contact, lower lateral forces would result due to the low viscosity of air. Like the “dragging hypothesis,” this is at odds with the data in Figure 6 which show lateral forces growing with normal vibration amplitude.

Figure 10c also shows clear evidence of period doubling. Period doubling is a well-known property of systems with hard contact [12]. It is a practical problem for us due to production of audible sub-harmonics: while the excitation frequency of 22.3 K Hz is in the ultrasonic range, the 11.15 KHz sub-harmonic is audible.

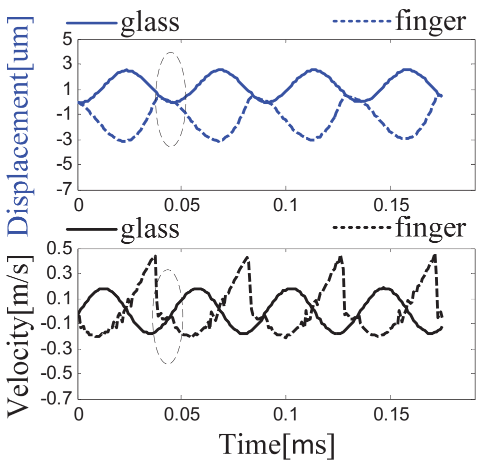

(a) Amplitude = 1.28 um

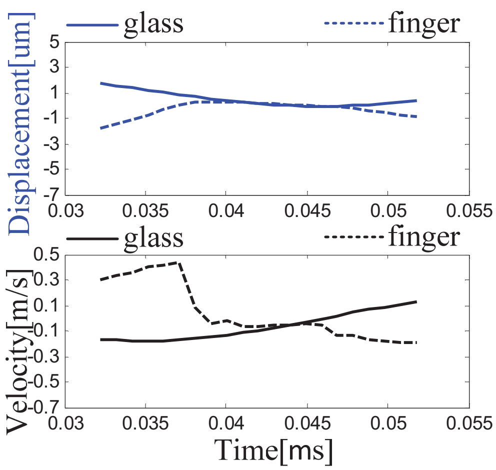

(b) Close-up of the period inside the dashed ellipse of (a)

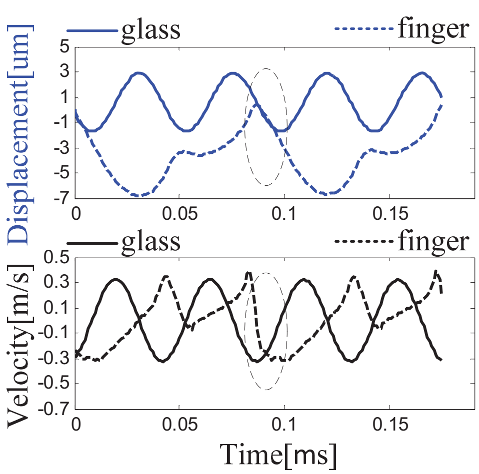

(c) Amplitude = 2.3 um; period doubling and squeeze film are evident.

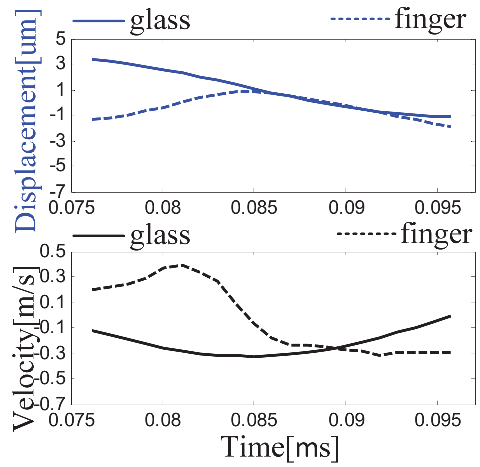

(d) Close-up of the period inside the dashed ellipse of (c)

Figure10. Impact between finger and glass at different normal vibration amplitudes (normal force ~ 0.5 N)

<u>Experiment 6 – Lateral and Normal motion of the surface</u>

Further insight into possible mechanisms of force production was gained by measuring the motion of the glass surface, including both normal and lateral components. The LDV can measure only motion along the axis of its laser. To measure the lateral component, a small piece of reflective tape was adhered to the top surface and the entire assembly was tilted as shown in Figure 11. By combining the measurements from Figure 11a (P_z) and Figure 11b (P_M), both components of motion could be determined.

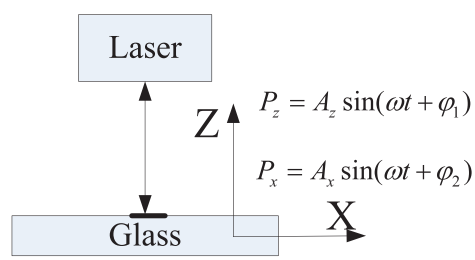

(a) Motion measurement when glass is horizontal

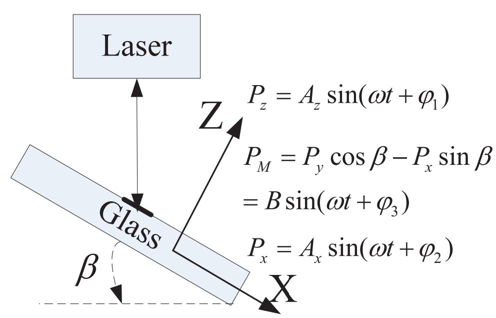

(b) Motion measurement when glass is tilted

Figure11. Two-axis motion measurement using the LDV

The peak-to-peak voltage across the piezo disks and piezo stack were set to 98 V and 192 V respectively, and the relative phase of these two driven voltages was set to 20°. In this case, the normal vibration and lateral vibration of LateralPaD were:

$$\begin{cases} P_z = A_z \sin(\omega t + \varphi_1) \\ P_x = A_x \sin(\omega t + \varphi_2) \end{cases} \tag{2}$$

Where A_z = 2246 nm, A_x = 786 nm, φ_1 = 14.6°, φ_2 = 194.3°, φ_1, φ_2 are the phases relative to the reference signal. The glass motion trajectory is shown in Figure 12. The relative phase of normal and lateral vibration was about 180° which means that the motion at peak force is essentially vibration along a straight line, tilted with respect to the vertical at an angle α:

$$\alpha = atan\left(\frac{A_x}{A_z}\right) = 19° \tag{3}$$

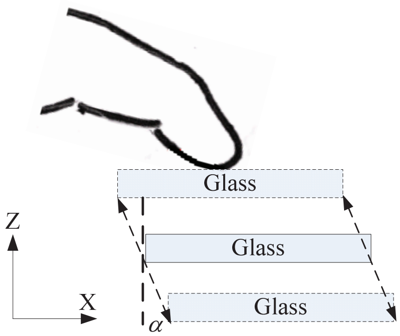

Figure 12. Impact model between finger and glass when motion of the glass surface is linear rather than elliptical

5 DISCUSSION

Experiment 6 revealed that maximum lateral force production occurs with straight line rather than elliptical surface motion. This suggests a mechanism of force production that may be quite different from “dragging.” It suggests instead that force is generated by a series of “tilted” impulses as shown in Figure 12. While dragging depends on kinetic friction, impulses may depend principally on static friction. The static friction coefficient of a fingertip on the glass surface was found to be ~0.7, corresponding to a friction cone of 35°. Because the tilt angle was found to be only 19 degrees (Eqn. 3), it seems likely that the tilted impulses lie within the static friction cone.

Further examination of this mechanism would benefit from a measurement of the relative *lateral* velocity between the LateralPaD surface and the fingertip; however, some corroboration can be found from TPaD data. With the TPaD, surface motion also occurs in a straight line, but that motion is purely vertical, not tilted. On the other hand, if the finger is moving, it should be possible to view the surface motion in the frame of the finger, and in that frame the motion would be tilted at the moment of impact. As such, when a finger is swept over the surface of the TPaD, it will experience a series of impulses. An effective coefficient of friction can be computed if the relative magnitudes of the lateral and normal components of the impulses can be determined. While we do not have a direct measure of the impulse magnitudes, we can estimate it by making two assumptions. The first assumption is that the tilt of the force impulse is collinear with the tilt of the relative velocity during impact. This is tantamount to assuming that the mechanical impedance of the fingertip is isotropic which seems reasonable since, at 22 KHz, the impedance is likely dominated by the inertia of the skin. The second assumption is that, in the normal direction, the relative velocity of impact is equal to the peak-to-peak velocity of the TPaD. This is a rough assumption stemming from the time domain data shown in Figure 10a and 10c. Fingertip and surface velocity are approximately 180 degrees out-of-phase and about the same amplitude. Moreover, the presumed collision (precipitous drop in fingertip velocity) occurs shortly after the peak in velocity. With these assumptions, the TPaD effective coefficient of friction can be computed as:

$$\mu_{effective} = \frac{v_{lateral}}{2\omega A_z} \tag{4}$$

Here, $v_{lateral}$ is the velocity of the finger, which was approximately 8 cm/sec for the data shown in Figure 4. Figure 13 overlays Eqn. 4 with the measured data of Figure 4. In Figure 13, the dashed curve is $\mu_{effective}$. While the fit is quite good over much of the range, it deviates for low and high values of normal amplitude. At low values of normal amplitude, this may occur because the static friction assumption is incorrect, and at high values of amplitude, this may occur due to the growing importance of a squeeze film, as indicated by Figure 10c.

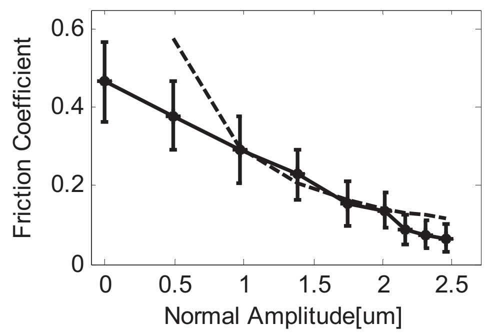

Figure 13. Comparison of tilted impulse model to measured friction coefficient for the TPaD

While additional experimental work is needed to verify and refine this model, an alternative model based solely on the existence of a squeeze film is simply not capable of explaining the gradual drop of friction coefficient with normal amplitude. As such, the data presented here make a strong case that tilted impacts play a role in the operation of both the TPaD and the LateralPaD.

As a final point, the data presented here indicate that the LateralPaD not simply a high frequency version of the ShiverPaD [10]. The ShiverPaD synchronizes relatively low frequency lateral oscillations to friction variations caused by turning a TPaD on and off. When the TPaD is off, the relative velocity will be principally in the lateral direction, a condition that never exists for the LateralPaD.

6 DEMONSTRATION OF FORCE AS A FUNCTION OF POSITION

For use as a surface haptic display, we wish to produce a lateral force as a software-generated function of fingertip position. Our prototype produces lateral forces only in one dimension, but a 2D version would be conceptually similar. As a 1D example we used the projected capacitance sensor and LateralPaD to create the force field associated with a virtual bump [2], as shown in Figure 14a. Depending on the finger's measured position, the lateral force production is modulated to create a force to the left or the right as appropriate. Figure 14b shows the measured force as a function of measured finger position. In Figure 14b, the light black curves are the raw force data and the dark black curve is the average. Figure 14c shows the "potential" of the displayed virtual bump, which defined as $\mathcal{V}(x) = -\int f_{Lateral}\,dx$. The finger is "repelled" away from the high potential position to low potential position. In practice, a distinct illusion of a bump is felt.

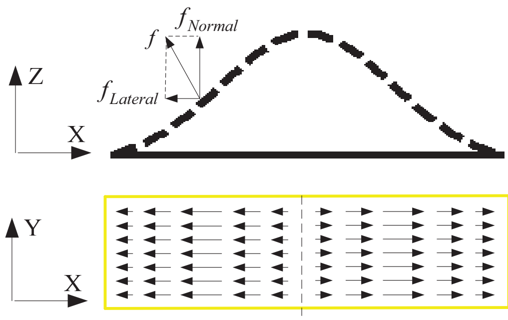

(a) The "bump" and its force field displayed on the LateralPaD

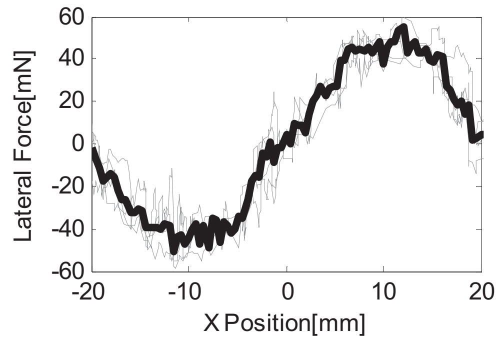

(b) Lateral force generated on bare finger

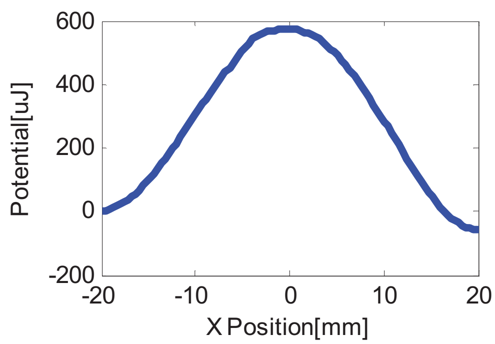

(c) Potential function

Figure 14. Force field used to display a virtual bump

7 Conclusions and Future Work

This paper presents the LateralPaD, a novel device capable of generating lateral force feedback on a bare finger touching a glass surface. Normal bending and lateral longitudinal resonances of a glass plate, and its driving piezo system, are arranged to occur at the same frequency. The relative phase of these vibrational modes is used to control the magnitude and direction of the lateral force. Force measurements presented here indicate that the lateral force coefficient increases with both normal and lateral vibrational amplitudes. This is surprising because, for a TPaD, the friction coefficient *decreases* with normal vibration amplitude. Force measurements also show that lateral force increases with average normal force, but less than linearly. For the prototype studied here, the maximum lateral force coefficient is about 0.13 and the maximum lateral force is around 70 mN.

Time domain measurements of finger and glass motion suggest that both squeeze film effects and impacts between the finger and glass surface may be involved. A "tilted impulse" model is proposed for the TPaD and LateralPaD and shown to produce reasonable predictions for the former. Future work will more fully explore the tilted impulse model for the LateralPaD. Among other things, we hope to explain the dependence of lateral force coefficient on normal vibration amplitude.

From the standpoint of developing practical surface haptic devices, several advances are needed. Devices with larger workspaces and smaller actuators need to be developed, devices with two axes of lateral force need to be developed, and larger forces must be generated by optimizing both materials and vibration characteristics.

Acknowledgements

This material is based upon work supported by the National Science Foundation under Grant No. IIS-0964075. The authors would like to thank Prof. Tom Royston and graduate student Zoujun Dai of University of Illinois at Chicago for access to and assistance with the LDV.

References

[1] Margaret Diane Rezvan Minsky. Computational Haptics: The Sandpaper System for Synthesizing Texture fora Force-Feedback Display. PhD dissertation, Massachusetts Institute of Technology, 1995.

[2] Gabriel Robles-De-La-Torre & Vincent Hayward. Force can overcome object geometry in the perception of shape through active touch. *Nature*, Vol. 412, pp: 445-448, 2001.

[3] Masaya Takasaki, Hiroyuki Kotani, Takeshi Mizunoe, et.al. Transparent Surface Acoustic Wave Tactile Display. *Proceedings of IEEE/RSJ International Conference on Intelligent Robots and Systems*, pp.3354-3359, Aug. 2005.

[4] Toshio Watanabe and Shigehisa Fukui. A Method for Controlling Tactile Sensation of Surface Roughness Using Ultrasonic Vibration, *Proceedings of IEEE International Conference on Robotics and Automation*, Vol. 1, pp: 1134-1139, May1995.

[5] Mélisande Biet, Frédéric Giraud, and Betty Lemaire-Semail. Implementation of Tactile Feedback by Modifying the Perceived Friction. *The European Physical J. Applied Physics*, Vol. 43, No. 1, pp. 123-135,July,2008.

[6] Laura Winfield, John Glassmire, J. Edward Colgate, and Michael Peshkin. T-PaD: Tactile Pattern Display through Variable Friction Reduction. *Proceedings of Second Joint EuroHaptics Conference and Symposium of Haptic Interfaces for Virtual Environment and Teleoperator Systems, WorldHaptics Conference,* 2007, pp: 421-426

[7] Akio Yamamoto, Shuichi Nagasawa, Hiroaki Yamamoto, et al. Electrostatic tactile display with thin film slider and its application to tactile telepresentation systems. *IEEE Transactions on Visualization and Computer Graphics*, Vol.12, No.2, pp: 168-177, March/April 2006.

[8] OlivierBau, Ivan Poupyrev, Ali Israr, et al. Teslatouch: electrovibration for touch surfaces. *Proceedings of the 23nd annual ACM symposium on User interface software and technology*, New York, NY, USA 2010, pp. 283-292

[9] Mélisande Biet, Frédéric Giraud, François Martinot et.al. A Piezoelectric Tactile Display Using Travelling Lamb Wave. *EuroHaptics Conference*, Paris, France, 2006.

[10] Erik C. Chubb, J. Edward Colgate, and Michael A. Peshkin. ShiverPaD: A Glass Haptic Surface That Produces Shear Force on a Bare Finger, *IEEE Transactions on Haptics*, Vol.3, No.3, pp: 189-198, 2010.

[11] Mélisande Biet, Frédéric Giraud, and Betty Lemaire-Semail. Squeeze Film Effect for the Design of an Ultrasonic Tactile Plate, IEEE Transactions on Ultrasonics, Ferroelectrics, and Frequency Control, Vol. 54, No. 12, December 2007

[12] Guckenheimer, J. & Holmes, P.-J. Nonlinear Oscillations, Dynamical Systems, and Bifurcations of Vector Fields, 3rd edition, Springer, 1991